Journal of Inflammation Research

Dovepress
open access to scientific and medical research

Open Access Full Text Article

ORIGINAL RESEARCH

The Molecular Mechanisms Study of Engeletin Suppresses RANKL-Induced Osteoclastogenesis and Inhibits Ovariectomized Murine Model Bone Loss

Mingzhe Feng[1,*], Lin Liu[2,*], Jiang Wang[1], Jialang Zhang[1], Zechao Qu[1], Yanjun Wang[3], Baorong He[1]

[1]Department of Spine Surgery, Honghui Hospital, School of Medicine, Xi'an Jiao Tong University, Xi'an, People's Republic of China; [2]Department of Critical Care Medicine, Honghui Hospital, School of Medicine, Xi'an Jiao Tong University, Xi'an, People's Republic of China; [3]Department of Emergency, Honghui Hospital, School of Medicine, Xi'an Jiao Tong University, Xi'an, People's Republic of China

*These authors contributed equally to this work

Correspondence: Baorong He, Department of Spine Surgery, Honghui Hospital, School of Medicine, Xi'an Jiao Tong University, Xi'an, People's Republic of China, Email baoronghespine@163.com; Yanjun Wang, Department of Emergency, Honghui Hospital, School of Medicine, Xi'an Jiao Tong University, Xi'an, People's Republic of China, Email wangyanjundoctor@163.com

Objective: Osteoclastogenesis, the process of osteoclast differentiation, plays a critical role in bone homeostasis. Overexpression of osteoclastogenesis can lead to pathological conditions, such as osteoporosis and osteolysis. This study aims to investigate the role of Engelitin in the process of RAW264.7 cell differentiation into osteoclasts induced by RANKL, as well as in a mouse model of bone loss following ovariectomy.

Methods: We used RANKL-stimulated RAW264.7 cells as an in vitro osteoclast differentiation model. The effects of Eng on morphological changes during osteoclast differentiation were evaluated using TRAP and F-actin staining. The effects of Eng on the molecular level of osteoclast differentiation were evaluated using Western blot and q-PCR. The level of reactive oxygen species was evaluated using the DCFH-DA staining method. We then used ovariectomized mice as a bone loss animal model. The effects of Eng on changes in bone loss in vivo were evaluated using micro-CT and histological analysis staining.

Results: In the in vitro experiments, Eng exhibited dose-dependent inhibition of osteoclast formation and F-actin formation. At the molecular level, Eng dose-dependently suppressed the expression of specific RNAs (NFATc1, c-Fos, TRAP, Cathepsin K, MMP-9) involved in osteoclast differentiation, and inhibited the phosphorylation of proteins such as IκBα, P65, ERK, JNK, and P38. Additionally, Eng dose-dependently suppressed ROS levels and promoted the expression of antioxidant enzymes such as Nrf2, HO-1, and NQO1. In the in vivo experiments, Eng improved bone loss in ovariectomized mice.

Conclusion: Our study found that Eng inhibited RANKL-induced osteoclast differentiation through multiple signaling pathways, including MAPKs, NF-κB, and ROS aggregation. Furthermore, Eng improved bone loss in ovariectomized mice.

Keywords: engeletin, RANKL, osteoclastogenesis, ROS, MAPKs

Introduction

Osteoporosis is a common and potentially debilitating systemic bone disease that is characterized by reduced bone mass and the degeneration of bone tissue. This disease can be caused by various factors such as age, hormonal imbalances, lack of physical activity, and certain medical conditions or medications. Ultimately, osteoporosis leads to increased bone fragility and susceptibility to fractures, which can result in significant morbidity and even mortality, particularly in older adults.[1] Bone mineral density (BMD) and T score measured by dual energy X-ray absorptiometry (DXA) were used to define osteoporosis by World Health Organization (WHO). T score refers to the SD score of bone mineral density (BMD) related to the peak bone mass of healthy young women. The lower the T score, the higher the risk of fracture. The T score of normal population was between −1 and 1. A T score between −1 and −2.5 indicates loss of bone mass; A T-score of less than −2.5 indicated the presence of osteoporosis.[2] Research has indicated that individuals typically reach their peak

Received: 14 December 2022
Accepted: 2 May 2023
Published: 24 May 2023

bone density at around age 25, when they are in good nutritional health. After this point, bone mass gradually decreases. Postmenopausal women and men over the age of 60 experience a significant acceleration in bone loss, putting them at high risk for osteoporosis. These groups have a significantly increased risk of spinal and hip fractures, with the risk being twice as high for spinal fractures and two and a half times as high for hip fractures compared to individuals of the same age with normal bone mass. Both spinal and hip fractures are associated with high treatment costs and significant rates of disability and mortality. Recovery from these types of fractures can be lengthy and challenging, and in some cases, patients may require long-term care and support. These factors can place a significant burden on individuals and families, as well as on healthcare systems and society as a whole.[3] It is therefore essential to identify and manage osteoporosis risk factors and to encourage preventative measures to reduce the risk of fractures.[4]

Osteoporosis patients also need to take medication for the prevention and treatment of osteoporosis. These medications can be roughly divided into three categories: 1. Anti-resorptive drugs: bisphosphonates, calcitonin, estrogen, selective estrogen receptor modulators, cathepsin K inhibitors, specific RANKL inhibitor; 2. Bone-forming drugs: parathyroid hormone, active vitamin D; 3. Dual-action drugs: strontium salt drugs. Studies have demonstrated that patients receiving treatment with these medications for osteoporosis exhibit a decreased risk of vertebral, total hip, and non-vertebral fractures and an increase in bone mineral density (BMD) values over time.[5] However, the long-term and widespread use of these drugs for the treatment of osteoporosis is limited due to some side effects or expensive prices. For example, bisphosphonates, as first-line drugs for the treatment of osteoporosis, have side effects such as atypical femur fractures and jaw necrosis, as well as uncertain efficacy after 5 years of use. Long-term high-dose use of teriparatide, a drug in the class of parathyroid hormone, carries a risk of developing osteosarcoma. Long-term use of strontium ranelate, which has a dual effect of inhibiting bone resorption and promoting bone formation, carries a certain risk of gastrointestinal side effects and venous thromboembolism. Additionally, the use of strontium ranelate also carries a risk of cardiovascular events and can even lead to drug-induced delayed onset multi-organ hypersensitivity syndrome.[6] Therefore, it is imperative to invest in research for new drugs to treat osteoporosis, with the aim of improving the current treatment regimen.

Under normal conditions, bones are dynamically renewing tissues that maintain normal bone mass and density by balancing the processes of bone resorption and bone formation.[7,8] When this balance is upset, it can lead to bone disorders such as osteosclerosis and osteoporosis.[10,9] Bone formation is accomplished by osteoblasts, while bone resorption is accomplished by osteoclasts. Osteoblasts differentiate from mesenchymal stem cells,[11] while osteoclasts are large multinucleated cells derived from hematopoietic monocyte/macrophage progenitor cells.[12] Over-activation of osteoclasts and abnormal bone resorption function are the cellular basis of osteoporosis formation. Therefore, osteoclasts are the therapeutic target for the prevention and treatment of osteoporosis. Receptor activator of nuclear factor kappa B ligand (RANKL) and macrophage colony-stimulating factor (M-CSF) are two major regulators of osteoclast differentiation.[9] M-CSF is a cytokine that is produced by fibroblasts, endothelial cells, macrophages, or dendritic cells. It can act on hematopoietic stem cells, promote their differentiation into osteoclast precursor cells, and enhance their proliferation. Additionally, M-CSF can upregulate the expression of receptor activator of NF-κB (RANK) in osteoclast precursor cells. RANK belongs to the tumor necrosis factor receptor superfamily and acts as a receptor for RANKL. RANKL, also known as tumor necrosis factor ligand superfamily member 11, is the ligand for RANK.[13–15] When soluble or membrane-bound RANKL binds to RANK, it results in receptor oligomerization. This process leads to the recruitment of several conjugator molecules, such as TNF receptor-associated factor 6 (TRAF6), to a specific site in the proximal portion of the RANK membrane.[16] TRAF6 plays an important role in mediating various signaling pathways involved in osteoclast differentiation and function, including NF-κB, MAPK, AP-1, Akt/PBK signaling pathways, and cytoskeleton rearrangement. Furthermore, studies have demonstrated that increasing the level of reactive oxygen species (ROS) in osteoclasts can enhance osteoclast formation and activation.[17,18] Therefore, the RANK/RANKL axis has become a crucial molecular target for our research on the prevention and treatment of osteoporosis.[19]

Smilax glabra Roxb also known as Tufuling in Chinese, refers to the rhizome of a plant in the Liliaceae family. More than 200 compounds, such as flavonoids, phenolic acids, stilbenes, organic acids, and phenylpropanoids have been identified from *Smilax glabra Roxb*. Among them, flavonoids, phenolic acids, and phenylpropanoids are the most extensively studied and recognized as the main active constituents. Pharmacological studies have demonstrated that the active compounds in *Smilax glabra Roxb* possess various pharmacological effects, such as anti-infective,[20] anti-

cancer,[21] anti-inflammatory,[22,23] antioxidant,[24,24] and cardiovascular protective activities.[26,27] Engeletin (Eng) is a dihydroflavonoid extracted from *Smilax glabra Roxb*. and it possesses a wide range of pharmacological effects. Studies have shown that Eng can alleviate osteoarthritis by inhibiting the MAPKs and NF-κB signaling pathways and eliminating intracellular reactive oxygen species (ROS).[24] However, it remains unclear whether Eng possesses anti-osteoclast differentiation effects. The present study aimed to investigate the effects of Eng on osteoclastogenesis using a RANKL-induced osteoclast differentiation model in vitro and an ovariectomy-induced osteoporosis female C57BL/6J mice bone loss model in vivo.

Materials and Methods

Regent and Antibodies

Eng was purchased from Target Mol (Boston, Massachusetts, USA) and diluted in dimethyl sulfoxide (DMSO, Sigma-Aldrich, St. Louis, MO, USA). Recombinant RANKL was obtained from PeproTech EC, Ltd. (London, U.K.). Dulbecco's modified Eagle's medium (DMEM) and fetal bovine serum (FBS) were purchased from Gibco (Rockville, MD, USA). The Cell Counting Kit-8 (CCK-8) was obtained from Dojindo (Japan). The TRAP staining kit was provided by Sigma Aldrich (Sydney, Australia). Primary antibodies for c-Fos (sc-271,243) and NFATc1 (sc-7294) were purchased from Santa Cruz Biotechnology (Santa Cruz, CA, USA). Antibodies against phospho-p38 (4511T), p38 (8690T), phospho-ERK (4370T), ERK (4695T), phospho-JNK (4668T), JNK (67096S), phospho-NF-κB p65 (3033T), NF-κB p65 (8242T), phospho-Iκbα (9246S), Iκbα (4812S), HO-1 (26416T) and NQO-1 (62262S) purchased from Cell Signaling Technology (Beverly, MA, USA). Antibody of Nrf2 (PA5-27,882) was obtained from Thermo Fisher Scientific (Waltham, MA, USA). β-actin antibody (A2228) was purchased from Sigma-Aldrich, Inc. (St. Louis, MO, USA).

Cell Culture

The RAW 264.7 cell line was obtained from the American Type Culture Collection (ATCC, Manassas, VA) and cultured in DMEM supplemented with 10% FBS, in an atmosphere of 5% CO2 and 95% humidity at 37°C. The cells were passaged up to the 10th to 15th passages, and the density was adjusted to 60%-70%, which is optimal for stimulating osteoclast differentiation. RAW264.7 cells were seeded in a 96-well plate at a density of 6.25×10^3 cells per well and cultured in DMEM with 10% FBS. After 12 h of incubation, the cells attached to the bottom of the plate and were used for further experiments. The original DMEM medium in the 96-well plate was removed and replaced with α-MEM culture medium supplemented with 10% FBS, 1% penicillin-streptomycin, and 50ng/mL RANKL, with or without varying concentrations of Eng (5, 10, 20, 40 and 60 μM). The cells were then incubated for 5 days until osteoclasts were formed. The experiment was repeated more than three times, with two teams conducting the experiment each time.

Ethical Use of Animals

All experimental procedures for mice studies were carried out in line with the regulations for experimental animal care of the Xi'an Jiaotong University Laboratory Animal Administration Committee, performed according to the Xi'an Jiaotong University Guidelines for Animal Experimentation and conformed to the Guide for the Care and Use of Laboratory Animals published by the US National Institutes of Health. The use of experimental animals was approved by the Xi'an Jiaotong University Laboratory Animal Administration Committee (2020–028).

Cytotoxicity Assay

RAW264.7 cells were seeded in 96-well plates at a density of 6.25×10^3 cells per well and allowed to incubate overnight. The next day, the cells were treated with different concentrations of engelitin (0, 5, 10, 20, 40 and 60μM) or DMSO. After 2 and 3 days, CCK-8 reagent was added and incubated in the incubator for 2 h. The absorbance of the solution was measured at 450 nm using a TriStar2 LB 942 Multimode Microplate Reader (Berthold Technologies Gmbh & Co. KG, Baden-Württemberg, Germany).

TRAP Staining

As described in 2.2, RAW264.7 cells were stimulated with RANKL (50ng/mL) and different concentrations of Eng for 5 days. Remove the medium from the 96-well plate and wash the cells three times with PBS. Fix the cells with 4% paraformaldehyde for 15 min and wash them again with PBS three times. Then, follow the staining instructions provided with the Trap kit. Osteoclasts were identified by counting the number of nuclei in cells observed under a Nikon ECLIPSE TE2000-S microscope. (Nikon, Japan). Cells were considered osteoclasts if they had three or more nuclei.

F-Actin Staining

The function of mature osteoclasts in bone resorption is dependent on the formation of F-actin podosome belts. Therefore, it is necessary to assess the impact of Eng on the formation of F-actin podosome belts. Cell cultures were carried out as described earlier, and then specific staining of F-actin was performed. First, the original culture medium was discarded, and the cells were carefully rinsed with 10% PBS for 3 times. Then, the cells were fixed with 4% PFA for 10 min and rinsed again with 10% PBS for 3 times. Next, the cells were permeabilized with 0.3% Triton X-100 at room temperature for 5 min, followed by the addition of an immunofluorescence dye. The cells were incubated in the dark at room temperature for 1 h, rinsed with 10% PBS, and then stained with DAPI for 5 min. After washing again with 10% PBS, the images were observed and collected under a fluorescence microscope (Nikon, Japan).

ROS Production Assay

Intracellular ROS levels are involved in the regulation of osteoclast differentiation, and excessive ROS production can promote osteoclastogenesis. To investigate the effect of Eng on RANKL-induced intracellular ROS levels during osteoclast differentiation, RAW264.7 cells were seeded at a density of 3×10^3 cells per well in 96-well plates and pre-treated with different concentrations of Eng for 24 h in the presence of 50 ng/mL RANKL. After removal of the cell culture medium from the well plate, the cells were incubated with diluted DCFH-DA(1:1000) in a cell incubator for 20 min. Subsequently, the cells were rinsed three times with serum-free medium in a careful manner. Finally, the fluorescence of DCF was measured using a fluorescence microscope (Nikon, Japan).

Western Blot

RAW264.7 cells were seeded at a density of 2×10^5 cells per well in a 6-well plate and incubated for 24 h. After that, cells were treated with or without different concentrations of Eng for 24 h before being stimulated with 50 ng/mL RANKL for a specific period of time. Total proteins were extracted from cells using RIPA lysis buffer (Invitrogen, USA) containing a mixture of protease and phosphatase inhibitors. The protein sample was centrifuged at 12,000 g for 10 min at 4°C, and the supernatant was collected. The concentration of the protein sample was determined with the BCA protein analysis kit (Thermo Scientific Pierce, USA). Afterwards, the proteins were separated by sodium dodecyl sulfate-polyacrylamide gel electrophoresis (SDS-PAGE) and transferred onto polyvinylidene difluoride (PVDF) membranes (Millipore, USA). The membranes were then incubated with 5% skim milk for an h to block any nonspecific immune responses. Next, the membrane was incubated with the corresponding primary antibody solution and gently shaken at 4°C for 12 h. After 12 h of adequate specific immune response, the membrane was washed three times with TBST solution. The membrane was then subjected to a specific immune reaction with the corresponding secondary antibody for 1 h. After the enhanced chemiluminescent reagent was added to the membranes, the immunoreactive protein bands were detected using the Western-Light chemiluminescent detection system (Applied Biosystems, USA). The band densities were analyzed using ImageJ software (version 1.8.0, National Institutes of Health, USA).

Real-Time Quantitative PCR (qPCR)

To evaluate the effect of Eng on osteoclast differentiation at the gene expression level, RAW264.7 cells were seeded in 6-well plates at a density of 2×10^5 cells per well and stimulated with RANKL in the presence or absence of Eng. Total RNA was extracted using TRIzol reagent (Thermo Fisher Science, USA) and used to synthesize complementary genes by quantitative reverse transcription polymerase chain reaction (QRT-PCR). The cDNA was amplified by SYBR Kit

Table 1 Primer Sequences for qPCR

Target Gene	Primer Sequence (5′-3′) Forward	Primer Sequence (5′-3′) Reverse
NFATc1	TCAGAGTGAGACCGAGAGGC	TGACATGCGGGGTGTGTG
c-Fos	TGTTCCTGGCAATAGCGTGT	TCAGACCACCTCGACAATGC
TRAP	TGTCCGCTTGAGGGTACATT	GCAGGACAGCCCTTAGCATC
Cathepsin K	CTGCGGCATTACCAACATGG	ACTGGAAGCACCAACGAGAG
MMP-9	GTTAGCCAGAAGCTGCGGT	GGGGAAGACCACAAAAGTCG

(TaKaRa, Japan) and ABI 7500 sequencing system (Applied Biosystems, USA). Osteoclast-specific genes and the internal control gene GAPDH were quantified using FastStart Universal SYBR Green Master (Rox, CO, USA). Primer sequences for osteoclast-related genes can be found in Table 1.

Ovariectomized Mouse Model

8-week-old female C57BL/6J mice were purchased from the Experimental Animal Center of Shaanxi Province (Xi'an, PR China), randomly divided into three groups (Sham group, OVX group and OVX + Eng group, n=5). After mice were anesthetized with tribromoethanol, the bilateral ovaries were removed from mice of all groups except the sham group. A week later, the mice in OVX + Eng group were intraperitoneally injected with 5 mg/kg Eng every other day, while the mice in SHAM and OVX groups were intraperitoneally administrated with DMSO (1% in normal saline) every other day. All mice were then sacrificed through cervical dislocation after 8 weeks. The femurs of mice were extracted for micro-computed tomography (micro-CT) scanning and immunohistochemistry.

Micro-CT Data Analysis

After sacrificing the experimental mice, the right femurs were fixed with 4% PFA for 24 hours, placed in 1.5 mL microcentrifuge tubes, and scanned using micro-CT (SKYSCAN 1172, Belgium). A region of interest (ROI) 0.5 mm above the distal femur growth plate, with a height of 2 mm, was selected for analysis of the trabecular bone. The scanning parameters were as follows: 60 kV of source voltage; 120μA of source current; 0.5 mm of AI filter; 12μm of pixel size; 180 degrees rotation step. After scanning, the device reconstruction software NRECON (V1.6.9.4) Obtain a cross-sectional view of the specimen. Bone mineral density (BMD), trabecular number (Tb. N), trabecular thickness (Tb.Th), trabecular space (Tb.Sp), and connectivity density (Conn.D) were analyzed using CTAn (V1.14.4) Software.

Histological Analysis

The femur was decalcified with 14% EDTA for 4 weeks and sliced the tissue of 4 μm which was embedded in paraffin. The region of interest was near the distal femoral bone marrow cavity. Next, haematoxylin and eosin (H&E) staining and TRAP staining were carried out to evaluate the histological changes of each group. The paraffin-embedded bone sections were deparaffinized, then soaked and fixed with TRAP fixative for 30 seconds. After slight drying, they were stained with TRAP staining solution for 1 hour and counterstained with either hematoxylin staining solution or methyl green staining solution for 5 min. The Nikon microscope (Nikon Corporation, Japan) was used to capture images. The number of osteoclasts was automatically scanned and calculated using ImageJ software. H&E staining was scanned by the Aperio Scanscope. Bone histological parameters were calculated by ImageJ software.

Statistical Analysis

Each experiment and data were repeated three times or more, and all data were given mean ± standard deviation (SD). Comparison between groups was performed by one-way ANOVA and t-test. Graph Pad Prism software was used for statistical analysis, and significant statistical difference was considered when the value $P<0.05$.

Result

Eng Suppresses the Differentiation of RANKL-Induced OCs Without Inducing Cytotoxicity

The chemical structure of Eng is shown in Figure 1A. To investigate the effects of Eng (as shown in Figure 1C–E on RANKL-induced OC differentiation, RAW264.7 cells were treated with varying concentrations of Eng in the presence of RANKL (50 ng/mL). The results showed that the group induced by RANKL had numerous TRAP-positive multinucleated osteoclasts, whereas increasing concentrations of Eng inhibited TRAP-positive multinucleated osteoclast formation in a dose-dependent manner. To assess the impact of Eng treatment on cell viability during RANKL stimulation, cell viability was evaluated at 48 h. We found that RAW264.7 cells treated with different concentrations of Eng (0, 2.5, 5, 10, 20, 40, and 60 μM) or DMSO had no effect on cell viability for 48h (Figure 1B). Eng demonstrated a dose-dependent inhibition of RANKL-induced osteoclast formation, and concentrations below 40 μM did not induce any cytotoxic effects.

Eng Inhibits F-Actin Podosome Belts

The formation of F-actin podosome belts is a crucial indicator of osteoclast bone resorption activity and is a distinct feature of mature osteoclasts. Upon RANKL stimulation, RAW264.7 cells differentiated into osteoclasts and formed the F-actin podosome belts structure, as verified by rhodamine-phalloidin staining. The results of our study indicate that treatment with Eng led to a dose-dependent decrease in both the number and morphology of F-actin podosome belts in osteoclasts (as shown in Figure 2A). Specifically, significant inhibition of F-actin podosome belts formation was observed at a concentration of 40 μM compared to other concentrations (Figure 2B).

Eng Reduces RANKL-Induced mRNA Expression of Osteoclast-Specific Genes

Additionally, the expression of osteoclast-specific genes, including NFATc1, c-Fos, TRAP, Cathepsin K and Mmp9 has been shown to be required for the maturation of osteoclasts. Real-time PCR was performed to investigate the effect of Eng on the expression of these osteoclast-specific genes. For this experiment, RAW264.7 cells were treated with 50 ng/mL RANKL in the absence or presence of different doses of Eng. As shown in Figure 3A, the mRNA expression levels of NFATc1, c-Fos, TRAP, Cathepsin K and Mmp9 were reduced in the presence of 10 20 and 40 μM Eng during RANKL-induced osteoclastogenesis. Therefore, these results suggest that Eng can dose-dependently attenuate the expression of osteoclast-specific genes in vitro.

Eng Represses RANKL-Induced Activation of NF-κB and MAPKs Pathways

During osteoclast differentiation, NFATc1 and c-Fos play essential roles as transcription factors downstream of the NF-κB and MAPKs signaling pathways. Upon stimulation with RANKL, the expression levels of NFATc1 and c-Fos in RAW264.7 cells were significantly increased. However, Eng was found to inhibit the high expression of both NFATc1 and c-Fos (Figure 3B and C). This is consistent with our Real-Time Quantitative PCR results (Figure 3A), which showed a dose-dependent inhibition of NFATc1 and c-Fos expression by Eng, with the most significant effect observed at a concentration of 40μM. Activation of NF-κB and MAPKs is crucial for the initial induction of NFATc1. As Eng was found to inhibit RANKL-induced NFATc1 expression, we conducted an investigation to determine if Eng reduced NFATc1 expression by decreasing the activation of NF-κB or MAPKs in RAW264.7 cells during osteoclast differentiation. We evaluated the protein levels of relevant molecules (including IκBα, P65, P38, JNK and ERK) in the NF-κB and MAPK signaling pathways. During osteoclast differentiation, the phosphorylation of P65 and IκBα increases. Our results (shown in Figure 4A and B) demonstrate that the levels of P-IκBα and P-P65 expressed in RAW264.7 cells increased after RANKL stimulation. What's interesting is that Eng demonstrated a dose-dependent inhibition of RANKL-induced phosphorylation of IκBα and P65. Here, we observed that RANKL treatment resulted in increased levels of phosphorylation of ERK, JNK, and P38, but this increase was significantly inhibited by Eng treatment in a time and concentration-dependent manner (Figure 4C–F). Thus, these data confirm that Eng can repress the NF-κB and MAPKs pathways in RANKL-induced osteoclasts in vitro.

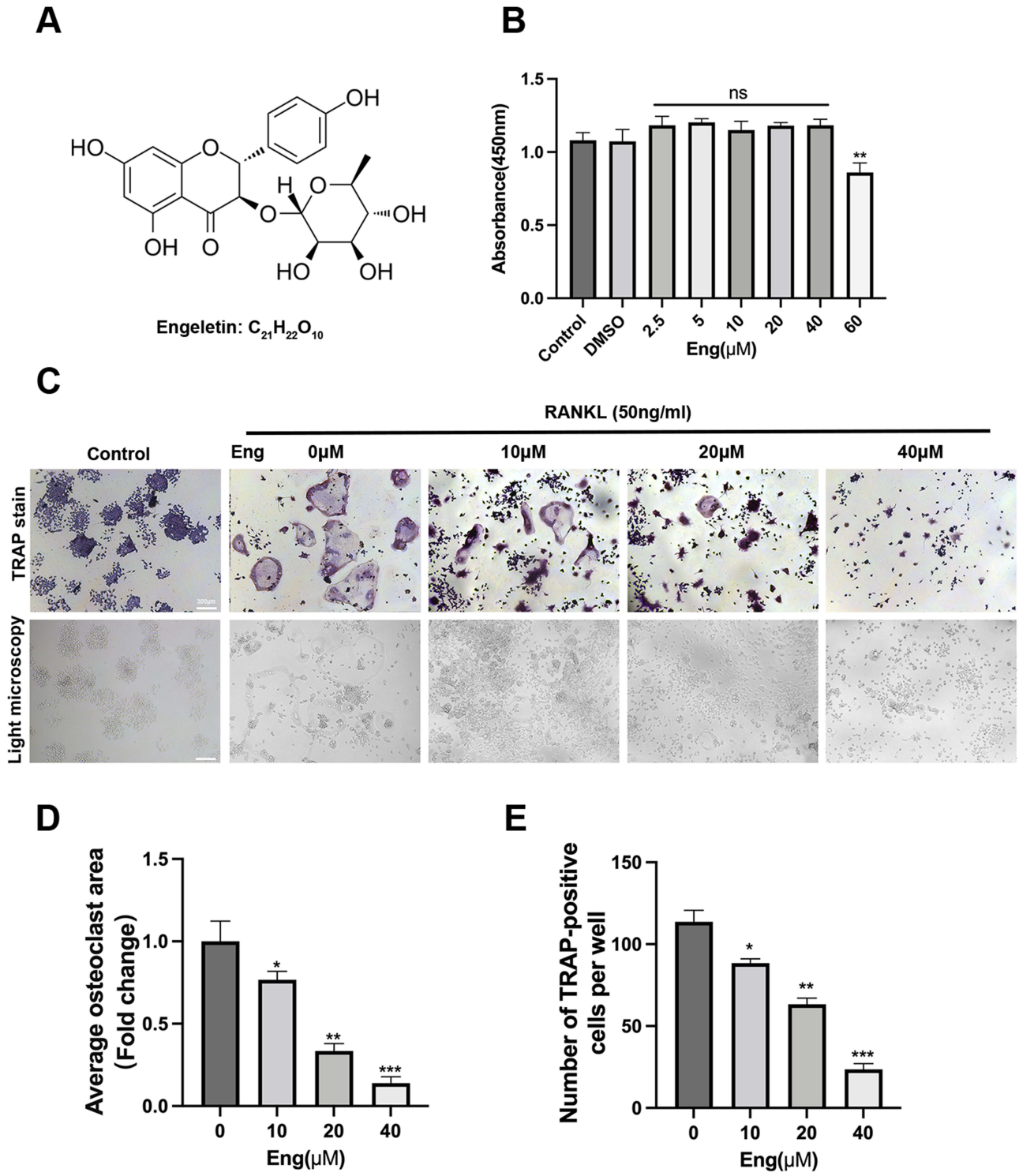

Figure 1 Eng inhibited RANKL-induced osteoclastogenesis in vitro in dose-dependent manner without cytotoxicity. (**A**) The chemical structure of Eng. (**B**) Effect of Eng on the viability of RAW264.7 cells. CCK-8 assay was used to detect the cytotoxicity of Eng. RAW264.7 cells were cultured for 48 and treated with different concentrations of Eng. Optical density values were measured at 450 nm. (**C**) Representative images of TRAP staining showing the osteoclast differentiation of RAW 264.7 induced by 50 ng/mL RANKL with or without Eng (0, 10, 20, 40μM), Scale bar=300 μm. (**D** and **E**) Area and number of TRAP-positive multinuclear cells (nuclei ≥3) were counted (n=3 per group). These data are expressed as mean ± SD. n = 3, **P* < 0.05, ***P* < 0.01 and ****P*<0.001 vs RANKL-induced group.

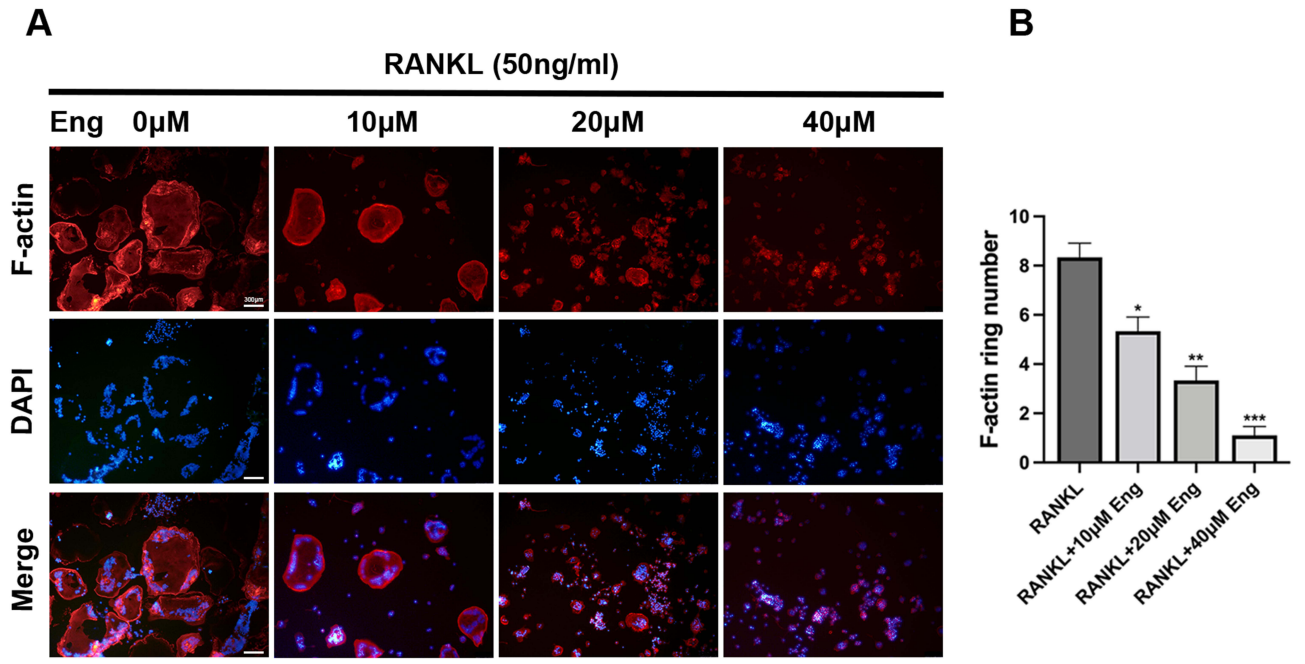

Figure 2 Eng inhibited the formation of F-actin. (**A**) RAW264.7 cells were treated with RANKL (50 ng/mL) and various concentrations of Eng (0, 10, 20, 40 μM) for 5 days. After fixing and permeabilizing the cells, F-actin was stained with phalloidin, and the nucleus was stained with DAPI. Representative images of osteoclasts with actin ring (in red) and cell nuclei (in blue) were obtained using a fluorescence microscope. Scale bar = 300 μm. (**B**) Quantification of F-actin ring number per osteoclast. These data are expressed as mean ± SD. n = 3, **P* < 0.05, ***P* < 0.01 and ****P*<0.001 vs RANKL-induced group.

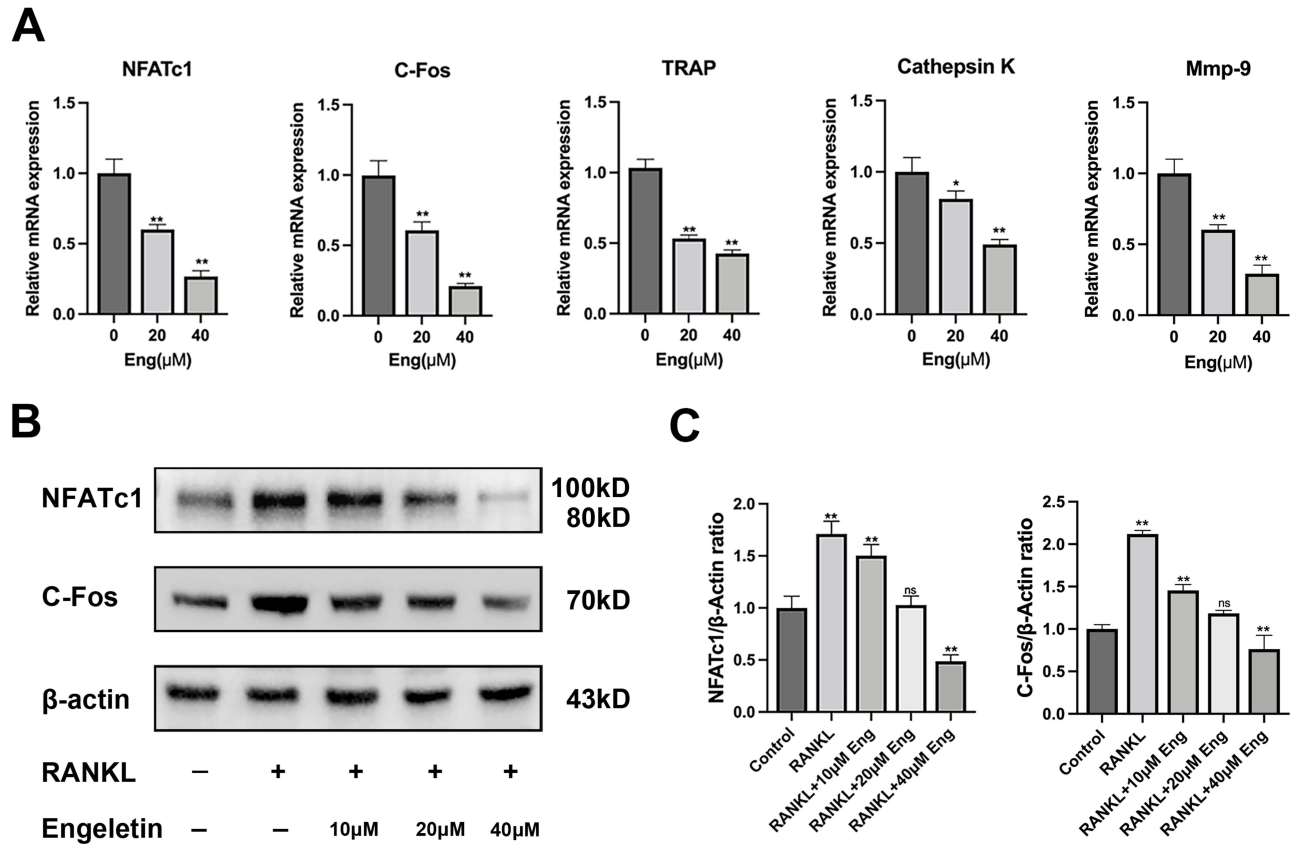

Figure 3 Eng inhibited the expression of c-Fos and NFATc1 and affected the expression of osteoclast-related mRNA. (**A**) Eng down-regulated of osteoclast-specific genes (NFATc1, c-Fos, TRAP, Cathepsin K, MMP-9). (**B**) RAW264.7 was treated with 50 ng/mL RANKL and different concentrations of Eng. Western blot was used to detect the expression levels of c-Fos and NFATc1. (**C**) The ratios of the intensity of NFATc1 or c-Fos relative to β-actin were determined using ImageJ. All bar charts are presented as mean ± SD; n=3. **P*<0.05, ***P*<0.01, ns: not statistically significant, vs control group.

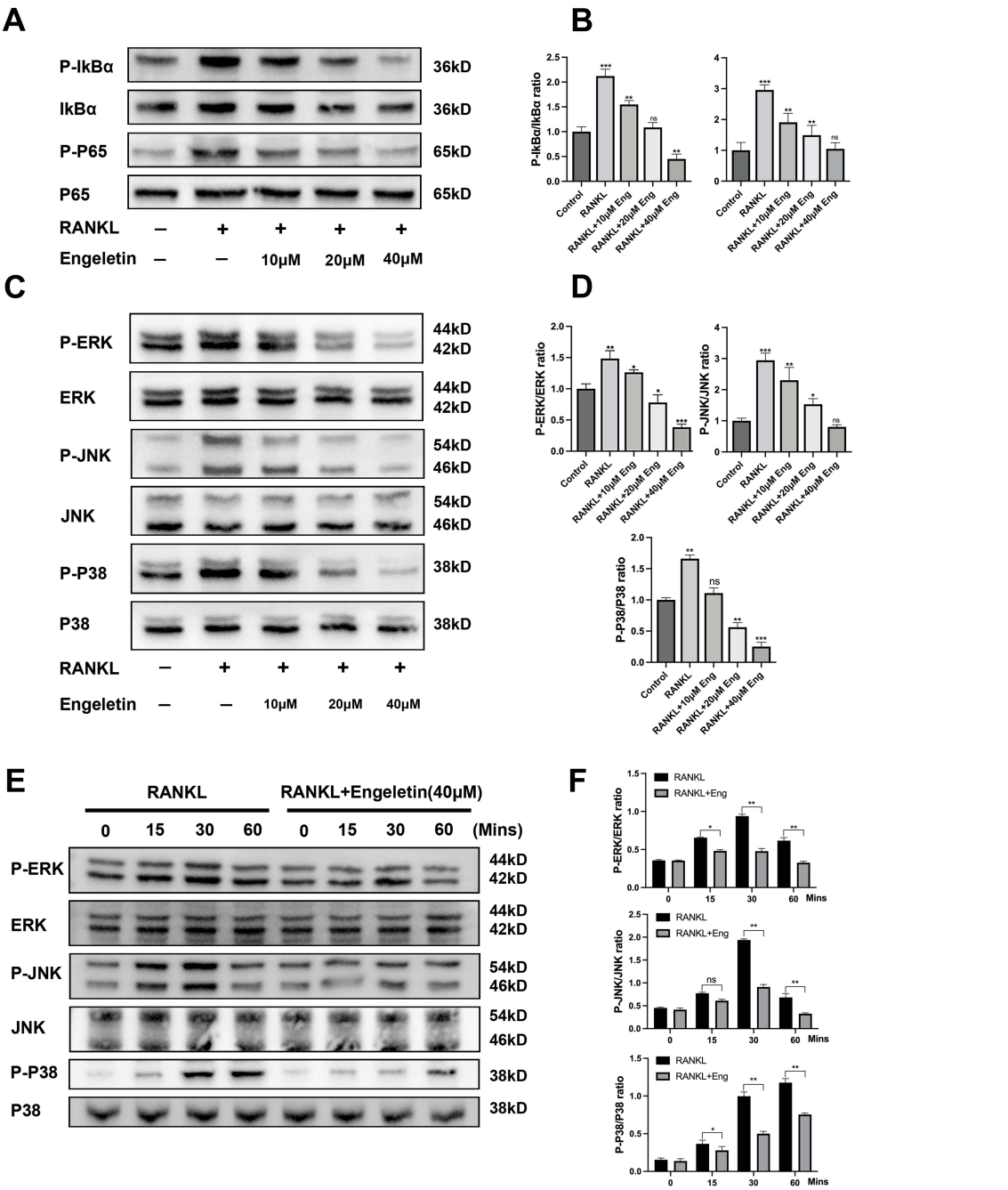

Figure 4 Eng inhibited the RANKL-induced NF-κB and MAPK signaling pathway. (**A**) RAW264.7 was treated with 50 ng/mL RANKL and different concentrations of Eng. Representative Western blotting images of the effects of Eng on IκBα and P65 phosphorylation. (**B**) The ratios of band intensity of IκBα and P65 phosphorylation relative to total IκBα and P65 were quantitatively determined (**C**) RAW264.7 was treated with 50 ng/mL RANKL and different concentrations of Eng. Representative Western blotting images of the effects of Eng on ERK, JNK, P38 phosphorylation. (**D**) The ratios of band intensity of ERK, JNK and P38 phosphorylation relative to total ERK, JNK and P38 were quantitatively. (**E**) RAW264.7 were pretreated with Eng (40 μM) for 60 min and stimulated by RANKL (50 ng/mL) for the indicated time points. (**F**) The ratios of phosphorylated ERK, JNK, and P38 bands to total ERK, JNK, and P38 bands at different time points were quantified. All bar charts are presented as mean ± SD; n=3. **P*<0.05, ***P*<0.01, ****P*<0.001, ns: not statistically significant.

Eng Negatively Regulated ROS Levels in vitro

ROS plays an important role in the normal metabolism of cells. It is worth noting that excessive ROS accumulation can stimulate osteoclast differentiation. Therefore, to investigate the effect of Eng on RANKL-induced ROS production, intracellular ROS levels were detected by DHE fluorescence staining as previously described. It is worth noting that while the fluorescence intensity increased in the RANKL group, the addition of Eng led to a dose-dependent decrease in

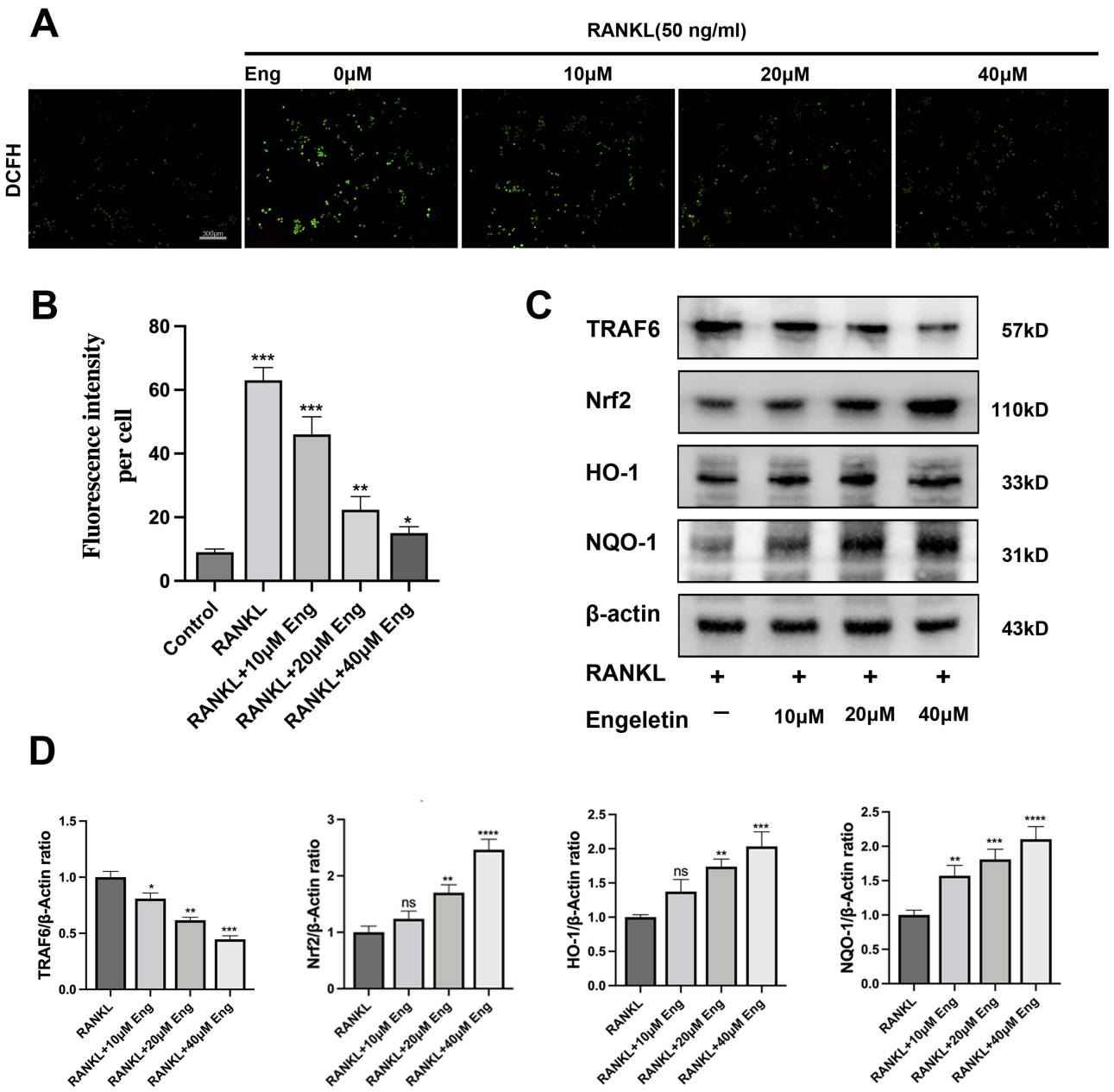

Figure 5 Eng inhibited RANKL-induced ROS activation and increased the expression of ROS scavenging enzymes. (**A**) RAW264.7 cells were induced with RANKL (50 ng/mL) and different concentrations of Eng (10, 20,40 μM) for 48 h, and then incubated with 5 μM DCFH-DA in the dark for 30 min. The fluorescence of DCF was observed under a laser confocal microscope. Scale bar = 300μm. (**B**) Quantification of DCF fluorescence intensity in an average per cell. (**C**) RAW264.7 were stimulated with RANKL (50 ng/mL) and different concentrations of Eng for 48 h. Representative Western blotting images of the effects of Eng on Nrf2, HO-1 and NQO-1 expression. (**D**) Quantification of the ratios of band intensity of Nrf2, HO-1, and NQO-1 relative to β-actin. All bar charts are presented as mean ± SD; n=3. **P*<0.05, ***P*<0.01, ****P*<0.001, ns: not statistically significant, vs RANKL group.

ROS fluorescence intensity (Figure 5A and B). Antioxidants are known to negatively regulate ROS levels, so we investigated whether Eng regulates ROS levels by modulating the production of antioxidants at the molecular level. The expression of nuclear factor erythroid 2-related factor 2 (Nrf2) and its regulated antioxidant enzymes, heme oxygenase-1 (HO-1) and NADPH: quinone reductase (NQO1), were detected by Western Blot. The Western Blot results demonstrated that Eng effectively increased the expression of antioxidant enzymes, such as Nrf2, NQO1, and HO-1 (Figure 5C and D).

Eng Attenuates Bone Loss in OVX Mice

To determine whether Eng could prevent in vivo bone loss caused by oestrogen deficiency, we used the OVX mice model, which mice postmenopausal osteoporosis. Micro-CT scanning of the right distal femur of the three groups of mice 8 weeks post-treatment revealed that the OVX groups experienced significant decreased trabecular bone volume compared with that of the sham control group, while bone loss in the Eng-treated group were significantly less compared to that of the OVX group (Figure 6A and B). This indicated that Eng positively affected the skeletal structure of OVX mice. Quantitative bone

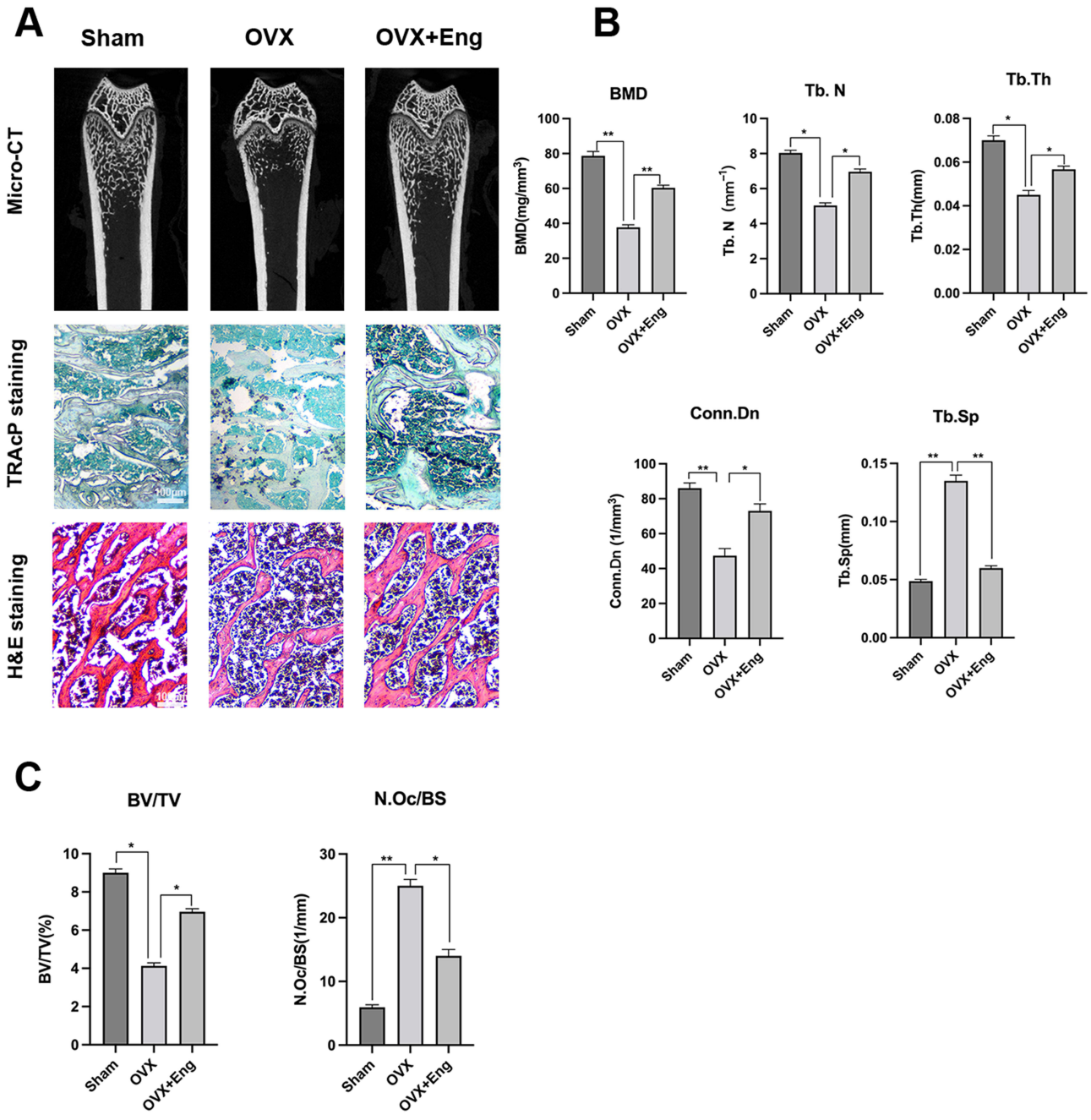

Figure 6 Eng prevents OVX-induced bone mass loss in vivo. All mice were randomly divided into three groups: Sham group (n=5), OVX group (n=5), and OVX+Eng (5 mg/kg) group (n=5). Bilateral ovariectomy was performed to induce osteoporosis under tribromoethanol anesthesia in OVX and OVX+Eng groups. For the mice of sham group, the ovaries were only exteriorized but not resected. All mice had 7 days recovery after the operations, then an intraperitoneal injection of Eng (5 mg/kg every other days for 8 weeks) was performed for the mice in the OVX+Eng group. The sham and OVX group mice were intraperitoneally injected with DMSO (1% in normal saline) as a vehicle control. (**A**) Images of micro-CT analysis and representative images of H&E, TRAP staining of decalcified bone sections. (**B**) Graphic representation of Bone mineral density (BMD), trabecular number (Tb. N), trabecular thickness (Tb. Th), trabecular space (Tb. Sp) and connectivity density (Conn.D), (n=5 per group). (**C**) Quantitative analyses of bone volume per tissue volume (BV/TV) and osteoclast number/bone surface (N. Oc/BS) in tissue sections (n=6 per group). All bar charts are presented as mean ± SD. **P*<0.05, ***P*<0.01, ns: not statistically significant, vs OVX group.

parameters further reflected that the Eng-treated group significantly increased BMD, Tb.N, Tb. Th and Conn.D, with decreased Tb. Sp (Figure 6B). Histological analysis further confirmed that OVX-induced bone mass loss was significantly reduced by the Eng treatment when compared with the OVX group. Quantification of H&E staining indicated that the bone surface and bone volume were well maintained in the Eng treatment group (Figure 6A and C). TRAP staining showed the osteoclast number per bone surface and osteoclast surface area per bone surface were decreased after Eng treatment when compared with the OVX group (Figure 6A and C).

Discussion

Excessive activation of osteoclasts is a key factor in the pathogenesis of many adult skeletal disorders, such as osteoporosis.[28,29] Therefore, targeting the downregulation of osteoclast differentiation or function is a promising approach for treating osteoporosis.[30,31] In this study, we present novel findings that demonstrate the inhibitory effects of Eng on osteoclast formation in vitro by regulating ROS activity and MAPKs, NF-kB signaling pathways. Additionally, we also show that Eng has a protective effect on OVX-induced bone loss in a mouse model of osteoporosis in vivo.

RAW264.7 cells are commonly used as osteoclast precursors and they can differentiate into osteoclasts in response to RANKL.[32] In the absence of stimulation, RAW264.7 cells only proliferate. After successful RANKL stimulation, RAW264.7 cells preferentially differentiate into osteoclasts. In our current study, we conducted a CCK-8 assay to determine the cytotoxicity of Eng at different concentrations ranging from 0 to 60μM. The results showed that Eng was not cytotoxic at these concentrations of 40 μM and below. We then investigated the effect of Eng on osteoclast differentiation and found that it had a dose-dependent inhibitory effect. To further confirm this, we stained and visualized F-actin belts, which are a signature structure of mature osteoclasts, and observed that Eng interfered with the formation of podosome belts, which further confirmed its inhibitory effect on osteoclast formation.

It has been extensively documented that the RANKL/RANK signaling pathway is crucial for the formation, maturation, and proper functioning of osteoclasts.[33] RANKL, a member of the tumor necrosis factor (TNF) superfamily, plays a critical role in signaling to induce osteoclast differentiation and facilitate the activation of precursor cells by interacting with its receptor RANK.[34] When RANKL binds to RANK, it recruits the adapter molecule TNF receptor-associated factor 6 (TRAF6), resulting in the activation of nuclear factor κB (NF-κB) and mitogen-activated protein kinases (MAPKs) signaling pathways. These pathways then activate transcription factors such as c-Fos and nuclear factor of activated T cells cytoplasmic 1 (NFATc1), which are crucial for osteoclast differentiation and function.[35] c-Fos is a critical regulator of RANKL-induced osteoclast formation, and is an important component of the AP-1 complex.[36] Studies have shown that c-Fos deficient mice develop osteosclerosis due to impaired osteoclast formation, which can be normalized by ectopic expression of c-Fos.[37] NFATc1, on the other hand, is a master regulator of the osteoclast transcriptome and is also regulated by c-Fos. NFATc1 plays a vital part in the formation and activity of osteoclasts and is known for its self-amplification to maintain robust expression.[38] The AP-1 complex containing c-Fos binds to the NFATc1 promoter and induces the expression of NFATc1.[39] Activated NFATc1 induces the expression of several osteoclast-specific genes, such as TRAP, Cathepsin K, and MMP-9, which are important for osteoclast formation and function.[40] Our Western blotting results demonstrated that Eng inhibited the RANKL-induced expression of c-Fos and NFATc1 in a dose-dependent manner. Similarly, the mRNA levels of c-Fos and NFATc1 were also inhibited by Eng in a dose-dependent manner. Notably, the expression of several osteoclast-specific genes induced by NFATc1 was also inhibited by Eng, which was expected based on the observed inhibition of NFATc1 expression.

The NF-κB signaling pathway, including IκBα and p65, is an important regulatory pathway during osteoclast formation. Typically, nuclear translocation of inactive NF-κB cannot take place until its inhibitor IκBα is degraded. IκBα phosphorylates and degrades gradually when upstream signals are stimulated. Without IκBα inhibition, NF-κB undergoes nuclear translocation to transmit the signal into the nucleus.[41] Previous knockout studies have shown that mice lacking both NF-κB dimers were unable to form osteoclasts normally, leading to severe osteopetrosis.[42] In the present study, we found that the addition of RANKL activated the IκBα and P65 signaling pathways. However, when RANKL and Eng were added together, Eng inhibited the phosphorylation of IκBα and P65. The binding of RANKL to RANK activates downstream signaling pathways, including the MAPK family members ERK, JNK, and P38.[9,43] The phosphorylation of these proteins promote the activation and translocation of c-Fos and AP-1, which are important regulators of

osteoclast formation and function. Previous studies have shown that inhibitors of P38, JNK, or ERK can inhibit osteoclast formation.[44,45] In this study, we observed that Eng inhibited the phosphorylation of ERK, JNK, and P38 in a dose and time-dependent manner upon RANKL stimulation. This suggests that Eng may suppress RANKL-induced osteoclast differentiation by blocking the ERK, JNK, and P38 signaling pathways.

Increasing evidence indicates that ROS production underlies various pathological conditions, such as inflammation and osteoporosis.[46] The Nrf2-Keap1 complex serves as a sensor for oxidative stress and regulates the expression of a wide array of antioxidant and cytoprotective genes.[47] In response to oxidative stress, Nuclear factor erythroid 2-related factor 2 (Nrf2) is released from Keap1 and translocates to the nucleus, where it forms heterodimers with small Maf proteins and binds to antioxidant response elements (AREs) in the promoter regions of target genes. This leads to the transcriptional activation of antioxidant enzymes and other cytoprotective genes, including Haem Oxygenase-1 (HO-1), NAD(P)H Quinone dehydrogenase 1 (NQO1), which play a critical role in protecting cells against oxidative stress.[48] In this study, we found that Eng dose-dependently inhibited the production of intracellular ROS induced by RANKL. Further investigation revealed that Eng increased the expression of Nrf2 protein and antioxidant enzymes HO-1 and NQO1. This suggests that Eng's inhibitory effect on osteoclast differentiation may be attributed to decrease ROS production and increase ROS clearance thereby suppressing RANKL-induced osteoclast formation.

Considering the inhibitory effects of Eng on RANKL-mediated osteoclast differentiation and function in vitro, we established an OVX mice model to further investigate whether Eng has potential therapeutic effect in vivo. The analysis of Micro-CT scanning, H&E staining and TRAP staining on the femoral samples indicated less bone loss, less osteoclast numbers and more trabecular bones after Eng treatment. The results suggest that Eng plays a protective role in preventing osteoclast formation and bone loss in OVX mice.

Our study demonstrates that Eng attenuates RANKL-induced osteoclast differentiation via multiple signaling pathways, including MAPKs, NF-κB, ROS aggregation, and the expression of related antioxidant enzymes and osteoclast differentiation-related genes in vitro. (Signal pathway is shown in Figure 7). In addition, the study showed that Eng restored BMD from OVX-induced bone destruction in vivo. However, our study has some limitations. In the in vitro experiments, we did not evaluate the effect of Eng on osteoclast bone resorption function using bone resorption assays. In the in vivo experiments, we did not evaluate the effect of Eng on osteoblasts. In summary, these findings shed light on the

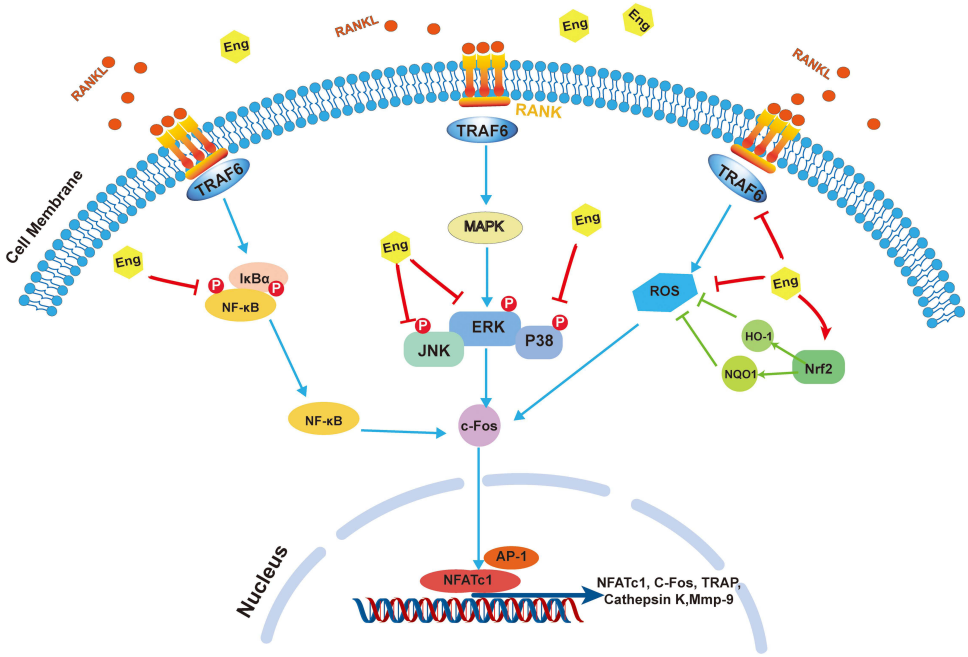

Figure 7 A proposed working model for the inhibition of Eng on osteoclastogenesis.

molecular mechanism underlying the anti-osteoclast effect of Eng and offer promising therapeutic ideas for the treatment of osteoclast-related bone diseases.

Data Sharing Statement

All data and materials were included in the manuscript.

Consent for Publication

The manuscript is approved by all authors for publication.

Acknowledgments

We thank Yunlong Zhang and Yingang Zhang for data collection and data analysis in the process of revising the manuscript.

Author Contributions

All authors made a significant contribution to the work reported, whether that is in the conception, study design, execution, acquisition of data, analysis and interpretation, or in all these areas; took part in drafting, revising or critically reviewing the article; gave final approval of the version to be published; have agreed on the journal to which the article has been submitted; and agree to be accountable for all aspects of the work.

Funding

This study was supported by a grant from Key project of National Science Foundation of China (82070909) and Key project of Natural Science Basic Research Plan of Shaanxi Province(2022JZ-43).

Disclosure

The authors declare that they have no competing interests in this work.

References

1. Cummings SR. Lifetime risks of hip, colles', or vertebral fracture and coronary heart disease among white postmenopausal women. *Arch Intern Med*. 1989;149(11):2445–2448.
2. Kanis JA, Melton LJ 3rd, Christiansen C, Johnston CC, Khaltaev N. The diagnosis of osteoporosis. *J Bone Miner Res*. 1994;9:1137–1141. doi:10.1002/jbmr.5650090802
3. Lane JM, Russell L, Khan SN. Osteoporosis. *Clin Orthop Relat Res*. 2000;372:139–150. doi:10.1097/00003086-200003000-00016
4. Srivastava M, Deal C. Osteoporosis in elderly: prevention and treatment. *Clin Geriatr Med*. 2002;18:529–555. doi:10.1016/S0749-0690(02)00022-8
5. Chen B, Meinertzhagen IA, Shaw SR. Circadian rhythms in light-evoked responses of the fly's compound eye, and the effects of neuromodulators 5-HT and the peptide. *J Comp Physiol A*. 1999;185:393–404. doi:10.1007/s003590050400
6. Rachner TD, Khosla S, Hofbauer LC. Osteoporosis: now and the future. *Lancet*. 2011;377:1276–1287. doi:10.1016/S0140-6736(10)62349-5
7. Parfitt AM. Bone remodeling and bone loss: understanding the pathophysiology of osteoporosis. *Clin Obstet Gynecol*. 1987;30:789–811. doi:10.1097/00003081-198712000-00004
8. Theill LE, Boyle WJ, Penninger JM. RANK-L and RANK: t cells, bone loss, and mammalian evolution. *Annu Rev Immunol*. 2002;20:795–823. doi:10.1146/annurev.immunol.20.100301.064753
9. Boyle WJ, Simonet WS, Lacey DL. Osteoclast differentiation and activation. *Nature*. 2003;423:337–342. doi:10.1038/nature01658
10. Asagiri M, Takayanagi H. The molecular understanding of osteoclast differentiation. *Bone*. 2007;40:251–264. doi:10.1016/j.bone.2006.09.023
11. Ducy P, Schinke T, Karsenty G. The osteoblast: a sophisticated fibroblast under central surveillance. *Science*. 2000;289:1501–1504. doi:10.1126/science.289.5484.1501
12. Teitelbaum SL. Bone resorption by osteoclasts. *Science*. 2000;289:1504–1508. doi:10.1126/science.289.5484.1504
13. Anderson DM, Maraskovsky E, Billingsley WL, et al. A homologue of the TNF receptor and its ligand enhance T-cell growth and dendritic-cell function. *Nature*. 1997;390:175–179. doi:10.1038/36593
14. Wong BR, Rho J, Arron J, et al. TRANCE is a novel ligand of the tumor necrosis factor receptor family that activates c-Jun N-terminal kinase in T cells. *J Biol Chem*. 1997;272:25190–25194. doi:10.1074/jbc.272.40.25190
15. Yasuda H, Shima N, Nakagawa N, et al. Identity of osteoclastogenesis inhibitory factor (OCIF) and osteoprotegerin (OPG): a mechanism by which OPG/OCIF inhibits osteoclastogenesis in vitro. *Endocrinology*. 1998;139:1329–1337. doi:10.1210/endo.139.3.5837
16. Lomaga MA, Yeh WC, Sarosi I, et al. TRAF6 deficiency results in osteopetrosis and defective interleukin-1, CD40, and LPS signaling. *Genes Dev*. 1999;13:1015–1024. doi:10.1101/gad.13.8.1015
17. Ha H, Kwak HB, Lee SW, et al. Reactive oxygen species mediate RANK signaling in osteoclasts. *Exp Cell Res*. 2004;301:119–127. doi:10.1016/j.yexcr.2004.07.035

18. Yip KH, Zheng MH, Steer JH, et al. Thapsigargin modulates osteoclastogenesis through the regulation of RANKL-induced signaling pathways and reactive oxygen species production. *J Bone Miner Res*. 2005;20:1462–1471. doi:10.1359/JBMR.050324
19. Wada T, Nakashima T, Hiroshi N, Penninger JM. RANKL-RANK signaling in osteoclastogenesis and bone disease. *Trends Mol Med*. 2006;12:17–25. doi:10.1016/j.molmed.2005.11.007
20. Tewtrakul S, Itharat A, Rattanasuwan P. Anti-HIV-1 protease- and HIV-1 integrase activities of Thai medicinal plants known as Hua-Khao-Yen. *J Ethnopharmacol*. 2006;105:312–315. doi:10.1016/j.jep.2005.11.021
21. She T, Zhao C, Feng J, et al. Sarsaparilla (Smilax Glabra Rhizome) extract inhibits migration and invasion of cancer cells by suppressing TGF-β1 pathway. *PLoS One*. 2015;10:e0118287. doi:10.1371/journal.pone.0118287
22. Wang C, La L, Feng H, et al. Aldose reductase inhibitor engeletin suppresses pelvic inflammatory disease by blocking the phospholipase C/Protein Kinase C-Dependent/NF-κB and MAPK Cascades. *J Agric Food Chem*. 2020;68:11747–11757. doi:10.1021/acs.jafc.0c05102
23. Zhao JW, Zheng CY, Wei H, Wang DW, Zhu W. Proapoptic and immunotoxic effects of sulfur-fumigated polysaccharides from Smilax glabra Roxb. in RAW264.7 cells. *Chem Biol Interact*. 2018;292:84–93. doi:10.1016/j.cbi.2018.07.009
24. Wang H, Jiang Z, Pang Z, et al. Engeletin protects against TNF-α-induced apoptosis and reactive oxygen species generation in chondrocytes and alleviates osteoarthritis in vivo. *J Inflamm Res*. 2021;14:745–760. doi:10.2147/JIR.S297166
25. Zhao X, Chen R, Shi Y, Zhang X, Tian C, Xia D. Antioxidant and anti-inflammatory activities of six flavonoids from smilax glabra Roxb. *Molecules*. 2020;25:5295. doi:10.3390/molecules25225295
26. Liu T, Li Y, Sun J, Tian G, Shi Z. Engeletin suppresses lung cancer progression by inducing apoptotic cell death through modulating the XIAP signaling pathway: a molecular mechanism involving ER stress. *Bio Pharmacot*. 2020;128:110221. doi:10.1016/j.biopha.2020.110221
27. Cai Y, Tu J, Pan S, et al. Medicinal effect and its JP2/RyR2-based mechanism of Smilax glabra flavonoids on angiotensin II-induced hypertrophy model of cardiomyocytes. *J Ethnopharmacol*. 2015;169:435–440. doi:10.1016/j.jep.2015.04.026
28. Plotkin LI, Bellido T. Osteocytic signalling pathways as therapeutic targets for bone fragility. *Nat Rev Endocrinol*. 2016;12:593–605. doi:10.1038/nrendo.2016.71
29. Udagawa N, Koide M, Nakamura M, et al. Osteoclast differentiation by RANKL and OPG signaling pathways. *J Bone Miner Metab*. 2021;39:19–26. doi:10.1007/s00774-020-01162-6
30. Qu Z, Zhang B, Kong L, et al. Receptor activator of nuclear factor-κB ligand-mediated osteoclastogenesis signaling pathway and related therapeutic natural compounds. *Front Pharmacol*. 2022;13:1043975. doi:10.3389/fphar.2022.1043975
31. Søe K, Delaisse JM, Borggaard XG. Osteoclast formation at the bone marrow/bone surface interface: importance of structural elements, matrix, and intercellular communication. *Semin Cell Dev Biol*. 2021;112:8–15. doi:10.1016/j.semcdb.2020.05.016
32. Kong L, Smith W, Hao D. Overview of RAW264.7 for osteoclastogensis study: phenotype and stimuli. *J Cell Mol Med*. 2019;23:3077–3087. doi:10.1111/jcmm.14277
33. Yasuda H. Discovery of the RANKL/RANK/OPG system. *J Bone Miner Metab*. 2021;39:2–11. doi:10.1007/s00774-020-01175-1
34. Ono T, Hayashi M, Sasaki F, Nakashima T. RANKL biology: bone metabolism, the immune system, and beyond. *Inflamm Regen*. 2020;40:2. doi:10.1186/s41232-019-0111-3
35. Elango J, Bao B, Wu W. The hidden secrets of soluble RANKL in bone biology. *Cytokine*. 2021;144:155559. doi:10.1016/j.cyto.2021.155559
36. Mognol GP, González-Avalos E, Ghosh S, et al. Targeting the NFAT:AP-1 transcriptional complex on DNA with a small-molecule inhibitor. *Proc Natl Acad Sci U S A*. 2019;116:9959–9968. doi:10.1073/pnas.1820604116
37. Fleischmann A, Hafezi F, Elliott C, Remé CE, Rüther U, Wagner EF. Fra-1 replaces c-Fos-dependent functions in mice. *Genes Dev*. 2000;14:2695–2700. doi:10.1101/gad.187900
38. Zhao Q, Wang X, Liu Y, He A, Jia R. NFATc1: functions in osteoclasts. *Int J Biochem Cell Biol*. 2010;42:576–579. doi:10.1016/j.biocel.2009.12.018
39. Wagner EF, Eferl R. Fos/AP-1 proteins in bone and the immune system. *Immunol Rev*. 2005;208:126–140. doi:10.1111/j.0105-2896.2005.00332.x
40. Yang D, Wan Y. Molecular determinants for the polarization of macrophage and osteoclast. *Semin Immunopathol*. 2019;41:551–563. doi:10.1007/s00281-019-00754-3
41. Lin B, Ke Q, Leaman DW, Goel V, Agarwal A. Regulation of RANKL-induced osteoclastogenesis by RING finger protein RNF114. *J Orthop Res*. 2018;36:159–166. doi:10.1002/jor.23654
42. Guo J, Ren R, Sun K, et al. PERK controls bone homeostasis through the regulation of osteoclast differentiation and function. *Cell Death Dis*. 2020;11:847. doi:10.1038/s41419-020-03046-z
43. Lee K, Chung YH, Ahn H, Kim H, Rho J, Jeong D. Selective Regulation of MAPK signaling mediates RANKL-dependent osteoclast differentiation. *Int J Biol Sci*. 2016;12:235–245. doi:10.7150/ijbs.13814
44. Thouverey C, Caverzasio J. Focus on the p38 MAPK signaling pathway in bone development and maintenance. *Bonekey Rep*. 2015;4:711. doi:10.1038/bonekey.2015.80
45. Koga Y, Tsurumaki H, Aoki-Saito H, et al. Roles of Cyclic AMP response element binding activation in the ERK1/2 and p38 MAPK signalling pathway in central nervous system, cardiovascular system, osteoclast differentiation and mucin and cytokine production. *Int J Mol Sci*. 2019;20:1346. doi:10.3390/ijms20061346
46. Agidigbi TS, Kim C. Reactive oxygen species in osteoclast differentiation and possible pharmaceutical targets of ROS-mediated osteoclast diseases. *Int J Mol Sci*. 2019;20:3576. doi:10.3390/ijms20143576
47. Bellezza I, Giambanco I, Minelli A, Donato R. Nrf2-Keap1 signaling in oxidative and reductive stress. *Biochim Biophys Acta Mol Cell Res*. 2018;1865:721–733. doi:10.1016/j.bbamcr.2018.02.010
48. Ulasov AV, Rosenkranz AA, Georgiev GP, Sobolev AS. Nrf2/Keap1/ARE signaling: towards specific regulation. *Life Sci*. 2022;291:120111. doi:10.1016/j.lfs.2021.120111